

# Enhanced photocatalytic decomposition of an organic dye under visible light with a stable LaFeO<sub>3</sub>/AgBr heterostructured photocatalyst

Yanren Song<sup>a</sup>, Su Xue<sup>a</sup>, Guanqiu Wang<sup>a</sup>, Jie Jin<sup>a</sup>, Qian Liang<sup>a</sup>, Zhongyu Li<sup>a,b,c,\*</sup>, Song Xu<sup>a,\*\*</sup>

<sup>a</sup> Jiangsu Key Laboratory of Advanced Catalytic Materials and Technology, School of Petrochemical Engineering, Changzhou University, Changzhou, 213164, PR China

<sup>b</sup> Advanced Catalysis and Green Manufacturing Collaborative Innovation Center, Changzhou University, Changzhou, 213164, PR China

<sup>c</sup> School of Environmental and Safety Engineering, Changzhou University, Changzhou, 213164, PR China

## ARTICLE INFO

### Keywords:

In-situ precipitation method  
LaFeO<sub>3</sub>/AgBr heterojunction  
Visible-light photocatalyst  
Z-scheme

## ABSTRACT

In this study, we synthesized a novel LaFeO<sub>3</sub>/AgBr heterojunction via an in-situ precipitation method. The composition, structure, and optical absorption properties of LaFeO<sub>3</sub>/AgBr were characterized by X-ray diffraction (XRD), scanning electron microscopy (SEM), transmission electron microscopy (TEM), and ultraviolet-visible diffuse reflectance spectroscopy. The photocatalytic activity of the LaFeO<sub>3</sub>/AgBr photocatalyst was determined based on the degradation of tetracycline and three types of dyes comprising methyl orange, rhodamine B (RhB), and malachite green. The photocatalytic performance of the LaFeO<sub>3</sub>/AgBr heterojunction was much better compared with that of the pure AgBr and LaFeO<sub>3</sub>. It should be noted that Ag nanoparticles were not present in the fresh LaFeO<sub>3</sub>/AgBr heterojunction. However, according to the XRD and TEM results obtained for 10%-LaFeO<sub>3</sub>/AgBr, Ag nanoparticles were generated in the LaFeO<sub>3</sub>/AgBr heterojunction during the photo-degradation process, which accelerated the separation of photoinduced carriers in the LaFeO<sub>3</sub>/Ag/AgBr system. Based on the detection of active species, we propose a Z-scheme photocatalytic and organic dye (RhB) photosensitization mechanism, which also considers the role of Ag nanoparticles in the separation of electrons and holes. The stability of the LaFeO<sub>3</sub>/AgBr heterojunction was also investigated, which showed that the incorporation of LaFeO<sub>3</sub> remarkably improved the photocatalytic activity as well as enhancing the stability of the LaFeO<sub>3</sub>/AgBr heterojunction by suppressing the photodecomposition of AgBr.

## 1. Introduction

In recent decades, the application of solar energy has been regarded as an effective method for addressing energy crises and environmental pollution [1–5]. In order to utilize solar energy, semiconductor photocatalysts, especially visible light-driven catalysts, have been developed to decompose organic pollutants [6–12], generate hydrogen [13], and inactivate bacteria [14] via chemical processes. However, the photocatalytic activity of traditional single-component photocatalysts depends mainly on the band structure. The ready recombination of photoinduced carriers and difficulty of generating electrons and holes directly decrease the photo-quantum yield. To overcome those bottlenecks that restrict the use of photocatalysts in contaminant removal, composite photocatalysts connected to a compound semiconductor have been investigated widely due to their effective interface transfer with electrons and holes [15–17]. In practice, an effective heterojunction greatly changes the energy band structure to prevent the

recombination of photogenerated electrons and holes, but it can also improve the reusability and photocatalytic activity of a single photocatalyst.

A suitable n-type semiconductor with high photocatalytic activity should be identified to develop a reliable heterostructure. AgBr is a novel visible light response semiconductor material with a narrow band-gap and it is widely considered to be suitable for the utilization of solar energy [18–20]. Unfortunately, AgBr alone is fairly unstable because the photogenerated electrons will bond with interstitial Ag<sup>+</sup> ions to form Ag<sup>0</sup> nanoparticles. Therefore, the photoinduced charge transfer behavior and low reusability of AgBr reduce the photoconversion efficiency [21]. Many studies have aimed to effectively ensnare the photoinduced electrons in order to prevent the association of electrons and Ag<sup>+</sup> [22–30]. Thus, multi-heterostructured photocatalysts have been developed to improve the stability and photocatalytic activity of AgBr for use in highly efficient and stable photocatalytic applications [31]. Moreover, photocatalysts and co-catalysts such as TiO<sub>2</sub> [32], hexagonal

\* Corresponding author. Jiangsu Key Laboratory of Advanced Catalytic Materials and Technology, School of Petrochemical Engineering, Changzhou University, Changzhou, 213164, PR China.

\*\* Corresponding author.

E-mail addresses: [zhongyuli@mail.tsinghua.edu.cn](mailto:zhongyuli@mail.tsinghua.edu.cn) (Z. Li), [cyanine123@163.com](mailto:cyanine123@163.com) (S. Xu).

<https://doi.org/10.1016/j.jpcs.2018.06.004>

Received 10 December 2017; Received in revised form 1 June 2018; Accepted 2 June 2018

Available online 05 June 2018

0022-3697/ © 2018 Elsevier Ltd. All rights reserved.

boron nitride (h-BN) [33], Fe [34], and graphene oxide (GO) [35] have been used to form AgBr-based composites, which have greater stability and higher photocatalytic activities than pure AgBr, probably because the interaction between AgBr and another semiconductor or Ag nanoparticles on the surfaces of composites can effectively suppress the recombination of photogenerated charge. Thus, developing a stable and efficient composite is necessary to enhance the photocatalytic activity of AgBr.

In addition,  $\text{LaFeO}_3$  has a typical  $\text{ABO}_3$ -type perovskite structure and it is a promising visible light photocatalyst with many advantages, such as high stability, non-toxicity, and low band gap energy [36]. However, the weak photogenerated charge separation of  $\text{LaFeO}_3$  yields negative photocatalytic activity. Fortunately, various strategies have been applied to address this problem, such as different preparation methods and doping modifications [37–39].  $\text{LaFeO}_3$  has been combined with many other photocatalysts such as  $\text{Ag}_3\text{PO}_4$  [40],  $\text{g-C}_3\text{N}_4$  [41], and  $\text{Fe}_2\text{O}_3$  [42] to significantly improve the photocatalytic activity. Considering that  $\text{LaFeO}_3$  possesses high stability and AgBr is an efficient photocatalyst, it is reasonable to expect that the  $\text{LaFeO}_3/\text{AgBr}$  heterojunction would exhibit increased light absorption with enhanced photocatalytic performance and stability.

In this study, we synthesized the  $\text{LaFeO}_3/\text{AgBr}$  heterojunction at room temperature via an in-situ precipitation method. Compared with pure  $\text{LaFeO}_3$  and AgBr, the novel heterostructured photocatalyst performed better with higher photocatalytic activity and greater stability during the photodegradation of dyes under irradiation by visible light. Finally, we propose a possible Z-scheme photocatalytic and organic dye (rhodamine B; RhB) photosensitization mechanism based on the experimental results obtained.

## 2. Experimental

### 2.1. Materials

$\text{Fe}(\text{NO}_3)_3 \cdot 9\text{H}_2\text{O}$ ,  $\text{La}(\text{NO}_3)_3 \cdot 6\text{H}_2\text{O}$ ,  $\text{AgNO}_3$ , KBr and  $\text{NH}_3 \cdot \text{H}_2\text{O}$  were purchased from Chemical Reagent Corp. All of the chemicals were of analytical grade and can be directly used as received without further purification.

### 2.2. Synthesis of $\text{LaFeO}_3$

Briefly, 2 mmol  $\text{Fe}(\text{NO}_3)_3 \cdot 9\text{H}_2\text{O}$ , 2 mmol  $\text{La}(\text{NO}_3)_3 \cdot 6\text{H}_2\text{O}$  and 4 mmol citric acid were dissolved in 50 mL of deionized water. After stirring the solution for 1 h, aqueous ammonia was added slowly to adjust the pH to 7. The mixture was heated to  $70^\circ\text{C}$  and stirred for another 4 h. The mixture was dried then at  $90^\circ\text{C}$  for 10 h to obtain the yellow xerogel. Finally, the precursor was calcined in air at  $500^\circ\text{C}$  for 2 h and the final product was designated as bare  $\text{LaFeO}_3$ .

### 2.3. Synthesis of $\text{LaFeO}_3/\text{AgBr}$

$\text{LaFeO}_3/\text{AgBr}$  was synthesized via an in-situ preparation method, with no light source. First, different stoichiometric amounts of  $\text{LaFeO}_3$  were dispersed in 40 mL of ethanol under ultrasonication for 1 h to obtain well dispersed  $\text{LaFeO}_3$ . Next, 1 mmol  $\text{AgNO}_3$  was dissolved in 5 mL of deionized water and 1 mmol KBr was also dissolved in 5 mL of deionized water. The  $\text{AgNO}_3$  and KBr solutions were added successively at an Ag:Br molar ratio of 1:1 to the  $\text{LaFeO}_3$  suspension under constant stirring. After addition, the mixtures were stirred vigorously for 5 h in the dark. The precipitates obtained were collected by filtration and washed several times with deionized water and absolute ethanol to dissolve any un-reacted raw materials. Finally, the mixtures were dried at  $60^\circ\text{C}$  for 6 h. The mass fractions of  $\text{LaFeO}_3$  in the  $\text{LaFeO}_3/\text{AgBr}$  heterojunction were controlled to 5 wt%, 10 wt%, and 15 wt%, which were designated as 5%- $\text{LaFeO}_3/\text{AgBr}$ , 10%- $\text{LaFeO}_3/\text{AgBr}$ , and 15%- $\text{LaFeO}_3/\text{AgBr}$ , respectively. Pure AgBr was prepared in the same

manner but without  $\text{LaFeO}_3$ .

### 2.4. Characterization

The crystalline catalyst samples were examined by X-ray diffraction (XRD) using a Rigaku D/Max-2500 PC X-ray diffractometer (Rigaku Co., Japan) with  $\text{Cu K}\alpha$  radiation,  $\lambda = 1.54056 \text{ \AA}$ , and the system operated at 40 kV and 100 mA. The purities of the as-prepared samples were investigated by energy dispersive X-ray spectroscopy (EDS) analysis. Transmission electron microscopy (TEM; JEM-2100) and scanning electron microscopy (SEM; JSM-6360LA, JEOL, Japan) were employed to measure the morphology and structure of the catalysts. Ultraviolet-visible light (UV-Vis) diffuse reflectance spectra were recorded with a UV-Vis scanning spectrophotometer (Shimadzu UV-2550). The photoluminescence (PL) spectra were determined for the samples using an Agilent Cary Eclipse. Moreover, PL probing spectroscopy was employed to detect  $\cdot\text{OH}$  radicals with terephthalic acid. Typically, the photocatalyst and terephthalic acid were added to  $1 \times 10^{-2} \text{ mol/L}$  NaOH solution and the concentration of terephthalic acid was controlled at  $5 \times 10^{-3} \text{ mol/L}$ .

### 2.5. Photocatalytic activity

The photocatalytic activities of the as-prepared materials were measured based on the degradation of methyl orange (MO), RhB, malachite green (MG), and tetracycline (TC) under a 1000-W Xe lamp with irradiation by visible light. In each photocatalytic experiment, 25 mg of the catalyst was added to 50 mL of aqueous dye solution (10 mg/L) or 50 mL of aqueous TC solution (20 mg/L). Subsequently, the mixtures were stirred in the dark for 0.5 h to reach an adsorption-desorption equilibrium between the sample and dye solution. Approximately 1.5 mL of each solution was then sampled at specific time intervals and centrifuged immediately to separate the photocatalyst powder. The supernatant solution was analyzed using a UV759 UV-Vis spectrometer (Shanghai Precision & Scientific Instrument Co. Ltd, China). The degradation efficiency of organic dyes was calculated as:  $E = (1 - C_t/C_0) \times 100\%$ , where  $C_0$  and  $C_t$  are the concentrations of the target pollution before and after illumination at time  $t$ , respectively.

## 3. Results and discussion

### 3.1. XRD analysis

Fig. 1 shows the XRD patterns obtained for  $\text{LaFeO}_3$ , AgBr, and the as-prepared  $\text{LaFeO}_3/\text{AgBr}$  samples with different proportions of  $\text{LaFeO}_3$ . Clearly, the original  $\text{LaFeO}_3$  sample peaks at  $2\theta = 22.6^\circ$ ,  $32.2^\circ$ ,  $39.7^\circ$ ,  $46.1^\circ$ , and  $57.4^\circ$  corresponding to the (101), (121), (220), (202), and (240) crystal planes of pure  $\text{LaFeO}_3$  could be indexed to the orthorhombic phase of  $\text{LaFeO}_3$  (JCPDS no. 88-0641). No other impurities

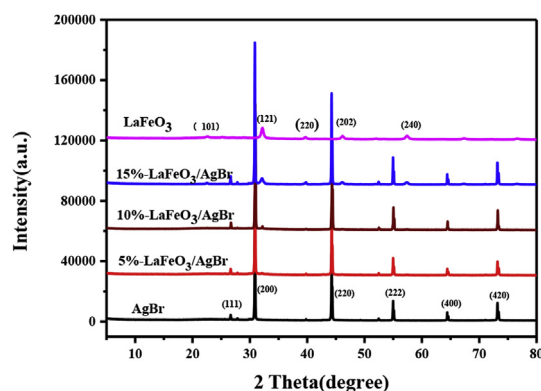


Fig. 1. XRD patterns obtained for the as-prepared samples.

Download English Version:

<https://daneshyari.com/en/article/7920004>

Download Persian Version:

<https://daneshyari.com/article/7920004>

[Daneshyari.com](https://daneshyari.com)